ARTICLE NO. 79-0280R

Turbulence Characteristics in the Near Wake of a Compressor Rotor Blade

B. Lakshminarayana* and B. Reynolds†
The Pennsylvania State University, University Park, Pa.

This paper is concerned with turbulence in the near wake of a rotating compressor blade. The variation of the axial, tangential, and radial turbulent stresses in the wake and their decay were measured with a triaxial hot-wire probe rotating with the rotor downstream of an axial-flow compressor. The turbulence intensities decay very rapidly in the near-wake region. The radial component of turbulent normal stress is found to be higher than the tangential and axial components. This is a consequence of the effect of rotation on the turbulence structure. A qualitative analysis is carried out to predict the effect of rotation on the turbulence structure. The results are in general agreement with the measured data.

Nomenclature

a, C_1, C_2, C_3, C_4 = constants
c = blade chord
e_1, e_2, e_3 = fluctuating hot-wire voltages
i = incidence angle relative to rotor blade chord
k = turbulent kinetic energy
L = length scale for the wake
ps = pressure side
p' = fluctuating pressure
Q = total velocity in the relative frame of reference
R = nondimensionalized radius (r/r_t)
r, θ, z = radial, tangential, and axial coordinate system (Fig. 1)
R_0 = Rossby number ($U_0/2\Omega L\cos\beta$)
s, n, r = streamwise, normal, and radial coordinate direction (Fig. 1)
ss = suction side
S = blade spacing
s = streamwise distance measured from the blade trailing edge
T_S, T_n, T_r = turbulent normal stress in streamwise ($\sqrt{\overline{u^2}}/Q_0$), normal ($\sqrt{\overline{v^2}}/Q_0$), and radial ($\sqrt{\overline{w^2}}/Q_0$) directions
T_r, T_θ, T_z = turbulent normal stress in radial, tangential, and axial directions, respectively (normalized by maximum axial velocity at the radius)
U_i = mean velocity component
U, V, W = mean velocity components in streamwise (s), normal (n), and radial (r) directions, respectively (Fig. 1)
u_i = fluctuating velocity component
u, v, w = fluctuating velocity in s, n, r system (Fig. 1)
$\overline{uv}/Q_0^2, \overline{vw}/Q_0^2$ = turbulent shearing stress in streamwise and radial directions, respectively
W_r, W_θ, W_z = mean velocity (relative) in r, θ, z system
w_r, w_θ, w_z = fluctuating velocity in r, θ, z directions (Fig. 1)
Y = tangential distance from the wake centerline nondimensionalized by blade spacing ($r\theta/S$, $\theta = 0$ at wake centerline, and Y is negative on the suction side and positive on the pressure side of the wake)
Z = axial distance from rotor blade trailing edge, nondimensionalized by chord length of rotor blade
β = flow outlet angle measured from axial direction
Ω^p = angular velocity component
ϵ_{ipq} = alternating tensor
ν = kinematic viscosity
g^{ij} = matric tensor
ϵ = dissipation
δ_{ij} = Kronecker delta
η_p, η_s = $r\theta/L_p$ and $r\theta/L_s$, respectively, with $\theta = 0$ at the wake centerline
τ_{sn}, τ_{rn} = streamwise and radial Reynolds stress, respectively ($\overline{uv}/Q_0^2$, $\overline{vw}/Q_0^2$)

Subscripts

c = wake centerline
m = maximum value
0 = freestream
t = tip
s, n, r = values along s, n, and r directions (Fig. 1)
p = pressure surface
s = suction surface

Superscripts

$\bar{()}$ = time average
$(')$ = time derivative

Introduction

BOTH the mean velocity defect and the turbulence properties of the wakes of rotor blades used in turbomachinery and other devices (e.g., propeller, helicopter, etc.) play a significant role in the noise generation, performance, and losses. This is especially true in turbomachinery stages, where the interaction effects generate not only the pure tone but also the broadband noise. Other effects that are equally significant are aerodynamic losses and inefficiency; vibration and flutter of the blade row; unsteady blade boundary layer, transition, and separation in the subsequent blade row; heat transfer; and cavitation in liquid-handling machinery. The main concern hitherto had been to

Presented as Paper 79-0280 at the AIAA 17th Aerospace Sciences Meeting, New Orleans, La., Jan. 15-17, 1979; submitted Jan. 25, 1979; revision received Jan. 28, 1980.

Index categories: Airbreathing Propulsion; Rotating Machinery; Jets, Wakes and Viscid-Inviscid Interactions.

*Professor of Aerospace Engineering. Associate Fellow AIAA.

†Graduate Assistant (presently Development Engineer, Avco Lycoming Division). Member AIAA.

investigate the velocity defect in the wake.[1-4] But recent theories and data have indicated that turbulence in the wake is also a major contributor to the unsteady forces, noise, inefficiency, and performance of the subsequent blade row. The objective of this work was to study the turbulence properties of the wake since there had been no previous attempts made to study the turbulence properties in a rotor wake.

The turbulence structure in the rotor wake is influenced by rotation, flow curvature, blade boundary layer, freestream turbulence, and pressure gradients, among other variables. The objective of this paper is to study the turbulence properties of the wake at various radial and downstream locations and to evaluate the decay characteristics. The properties measured are three components of turbulent normal stresses, streamwise and radial shear stresses, as well as spectrum of turbulent energy.

This paper is a continuation of an earlier paper[4] in which the measurement technique as well as the mean velocity properties were reported.

An attempt is made to provide a qualitative analysis of the effects of rotation on the turbulence structure in the rotating boundary layers and wakes.

Qualitative Analysis on the Effects of Rotation on Turbulence

The experimental investigation reported in Ref. 5 reveals that the effect of rotation on turbulence as well as mean velocity profiles in a rotor blade boundary layer is substantial. There are some structural changes in turbulence due to this additional force. Even though the rotor wake is not directly influenced by the rotation, the indirect influence arises due to the "history effect" via the blade boundary layer from which the wake was formed. The near-wake characteristics of a rotor wake can thus be expected to be different from those of an airfoil or a cascade wake. Some preliminary work on this effect, applicable to a rotor with axial relative flow (blade set in the axial direction) was cited in Ref. 6. The model used in Ref. 6 was not a practical configuration and the effect of rotation on the wake development was small.

The qualitative analysis presented here is applicable to any arbitrary rotor. It should be emphasized that the objective of this analysis is to evaluate, qualitatively, the effect of rotation on turbulence structure and thus provide the basis for the development of turbulence models for inclusion in the numerical analysis of shear layers subjected to rotation.

The Reynolds stress equation in a rotating curvilinear coordinate system[7] is

$$\overline{u_iu_k} + (\overline{u_iu_k})_{,j}U^j = -(\overline{u_ku^j}U_{i,j} + \overline{u_iu^j}U_{k,j}) - (\overline{u_iu_ku^j})_{,j} - 2\Omega^p(\overline{u_ku^q}\epsilon_{ipq} + \overline{u_iu^q}\epsilon_{kpq}) - (\overline{u_kp'_{,i}} + \overline{u_ip'_{,k}})/\rho - 2\nu g^{\ell j}\overline{u_{k,\ell}u_{i,j}} \quad (1)$$

The first two terms on the left side of Eq. (1) are the local variation of time-averaged stress and the convection of stress by mean flow, respectively. The terms in parentheses on the right side of the equation are, respectively, the production, the supression, the redistribution due to rotation, the redistribution due to pressure fluctuation, and the viscous dissipation of turbulence.

The Reynolds stress equation is intractable unless some simplifying assumptions are made, and the dissipation and diffusion terms are suitably modeled. These assumptions are:

1) The flow is statistically steady.

2) The radius of the rotor is large compared to wake or boundary-layer thickness ($L \ll r$). All other curvature terms are also neglected.

3) The term $(\overline{u_iu_ku^j})_{,j}$ is small.

4) The convection term is small. It should be emphasized here that at the trailing edge the boundary-layer assumptions are valid. Since the interest lies in the "history effect" on the properties of the near wake, this is a practically realistic assumption to make.

5) The pressure strain term in Eq. (1) is given by Rotta's[8] correlation

$$(\overline{u_kp'_{,i}} + \overline{u_ip'_{,k}})/\rho = \frac{C_1\epsilon}{k}(\overline{u_iu_k} - \frac{2}{3}\delta_{ik}k) + C_2(P_{ik} - \frac{2}{3}\delta_{ik}P) \quad (2)$$

where P_{ik}, the production by mean stress, is

$$P_{ik} = -(\overline{u_ku_j}U_{i,j} + \overline{u_iu_j}U_{k,j}) \quad (3)$$

6) The dissipation term in Eq. (2) is modeled assuming that the motion is isotropic[9]

$$2\nu g^{\ell j}\overline{u_{k,\ell}u_{i,j}} = \frac{2}{3}\delta_{ik}\epsilon \quad (4)$$

7) In the turbulence energy equation [derived by contracting the indices in Eq. (1)], the production term is assumed to be equal to dissipation.

These models and approximations reduce Eq. (1) to (in Cartesian form since curvature terms are neglected)

$$0 = P_{ik} - 2\Omega_p(\overline{u_ku_q}\epsilon_{ipq} + \overline{u_iu_q}\epsilon_{kpq}) - C_1\frac{\epsilon}{k}(\overline{u_iu_k} - \frac{2}{3}\delta_{ik}k) - C_2(P_{ik} - \frac{2}{3}\delta_{ik}\epsilon) - \frac{2}{3}\delta_{ik}\epsilon \quad (5)$$

The most suitable coordinate system for the analysis of the rotor wake is the s,n,r system shown in Fig. 1. Here, s is along the streamwise direction (on the cylindrical plane) at the wake centerline, n is normal to s, and r is in the radial direction. The corresponding velocities are also shown in Fig. 1. The vector Ω^p is in the z direction with components $\Omega_s = \Omega\cos\beta$ and $\Omega_n = -\Omega\sin\beta$.

In this coordinate system V and W are small compared to U and

$$P = \epsilon = (-\overline{uv})\frac{\partial U}{\partial n} + (-\overline{vw})\frac{\partial W}{\partial n} \quad (6)$$

Retaining only the dominant terms, the component form of Eq. (5) in this coordinate system reduces to the following

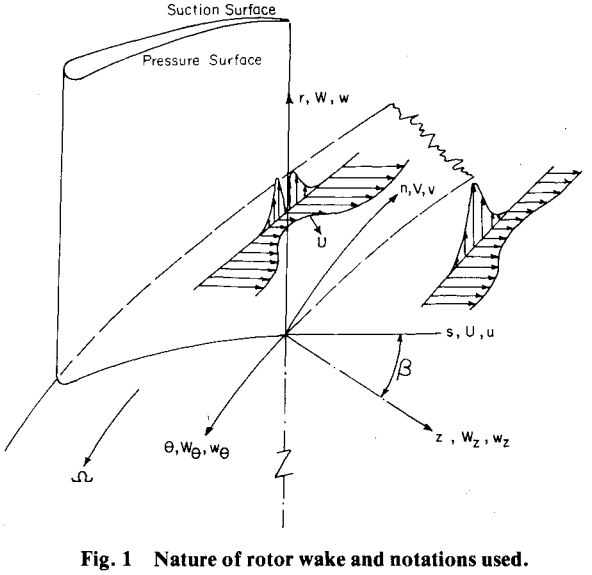

Fig. 1 Nature of rotor wake and notations used.

expressions:

$$C_1 = \frac{\epsilon}{k}\overline{u^2} = C_3(-\overline{uv})\frac{\partial U}{\partial n} + C_4(-\overline{vw})\frac{\partial W}{\partial n} - (\overline{uw})2\Omega\sin\beta \tag{7}$$

$$C_1\frac{\epsilon}{k}\overline{v^2} = C_4\epsilon - (-\overline{vw})2\Omega\cos\beta \tag{8}$$

$$C_1\frac{\epsilon}{k}\overline{w^2} = C_3(-\overline{vw})\frac{\partial W}{\partial n} + C_4(-\overline{uv})\frac{\partial U}{\partial n} + 2\Omega\sin\beta(-\overline{uw}) + 2\Omega\cos\beta(-\overline{vw}) \tag{9}$$

$$C_1\frac{\epsilon(-\overline{uv})}{k} = (1-C_2)\overline{v^2}\frac{\partial U}{\partial n} + 2\Omega\sin\beta(-\overline{vw}) + 2\Omega\cos\beta(-\overline{uw}) \tag{10}$$

$$C_1\frac{\epsilon(-\overline{vw})}{k} = (1-C_2)\overline{v^2}\frac{\partial W}{\partial n} - 2\Omega\sin\beta(-\overline{uv}) - 2\Omega\cos\beta(\overline{w^2}-\overline{v^2}) \tag{11}$$

$$C_1\frac{\epsilon(-\overline{uw})}{k} = -(1-C_2)\left[(-\overline{uv})\frac{\partial W}{\partial n} + (-\overline{vw})\frac{\partial U}{\partial n}\right] + 2\Omega\sin\beta(\overline{u^2}-\overline{w^2}) \tag{12}$$

where $C_3 = (2-2C_2+C_1)/3$ and $C_4 = (C_1+C_2-1)/3$.

The first three equations are the components of normal stresses in s, n, and r directions, respectively, and the last three equations are turbulent shear stresses in s, r, and n directions, respectively.

Using Eqs. (7-12), a qualitative estimate of the change in turbulence quantities for various cases can be made. In doing so, the constants employed in Ref. 10 for the two-dimensional, nonrotating case are used. These are $C_1 = 2.5$, $C_2 = 0.4$, hence $C_3 = 1.23$ and $C_4 = 0.633$.

Case 1: Stationary Two-Dimensional Flow ($\Omega = 0 = W$)

From Eqs. (7) and (9-11) the ratios of radial to streamwise normal and shear stresses are given by, respectively,

$$\overline{w^2}/\overline{u^2} = 0.514, \quad \overline{vw}/\overline{uv} = 0 \tag{13}$$

Case 2: Stationary Three-Dimensional Flow ($\Omega = 0$)

The ratio of the radial to streamwise shearing stress is given by,

$$\frac{(-\overline{vw})}{(-\overline{uv})} = \frac{\partial W/\partial n}{\partial U/\partial n} \tag{14}$$

This equation represents the standard assumption made in the numerical analysis of three-dimensional turbulent boundary layers (e.g., Ref. 11).

The ratio of the radial (or crosswise) to streamwise normal stresses is

$$\frac{\overline{w^2}}{\overline{u^2}} = \frac{1.23(-\overline{vw})\partial W/\partial n + 0.633(-\overline{uv})\partial U/\partial n}{1.23(-\overline{uv})\partial U/\partial n + 0.633(-\overline{vw})\partial W/\partial n} \tag{15}$$

Therefore, the ratio of the normal stresses is strongly dependent on the radial shear stress as well as the radial velocity gradient. For weak three-dimensional flows, these equations reduce to Eq. (13).

Case 3: Rotating Boundary Layers and Wakes with Small Radial Flow ($W \ll U$)

The ratio of radial to streamwise normal stress in this case can be approximated to,

$$\frac{\overline{w^2}}{\overline{u^2}} = \frac{C_4(-\overline{uv})\partial U/\partial n + 2\Omega\sin\beta(-\overline{uw}) + 2\Omega\cos\beta(-\overline{vw})}{C_3(-\overline{uv})\partial U/\partial n - 2\Omega\sin\beta(-\overline{uw})} \tag{16}$$

The effect of rotation can be expressed in terms of the Rossby number, which is the ratio of the inertial to Coriolis force, given by,

$$R_0 = U_0/\Omega L\cos\beta$$

where L is the characteristic length scale of the shear layer and $\Omega\cos\beta$ is the component of rotation in the U direction.

Furthermore $\partial U/\partial n = aU_0/L$, where L is a length scale. Therefore, Eq. (16) can be expressed as,

$$\frac{\overline{w^2}}{\overline{u^2}} = \frac{C_4(-\overline{uv}) + (-\overline{uw})\tan\beta/R_0a + (-\overline{vw})/R_0a}{C_3(-\overline{uv}) - (-\overline{uw})\tan\beta/R_0a}$$

In turbomachinery, R_0 is large and therefore the above equation can be simplified to,

$$\frac{\overline{w^2}}{\overline{u^2}} = \frac{C_4}{C_3} + \left(\frac{C_4}{C_3}+1\right)\frac{\tan\beta}{R_0aC_3}\frac{(-\overline{uw})}{(-\overline{uv})} + \frac{(-\overline{vw})}{(-\overline{uv})}\frac{1}{C_3aR_0} \tag{17}$$

This clearly shows that if $(-\overline{uw})$, $(-\overline{uv})$, and $(-\overline{vw})$ are of the same sign, the radial component of normal stress increases with an increase in rotation (decrease in the Rossby number). This trend has been observed in a boundary layer.[5] Therefore, the rotor boundary layer and wake should have a substantially higher radial component of turbulent normal stress as compared to a corresponding stationary case. Thus the effect of rotation is to redistribute the turbulent energy in the streamwise and radial directions, even though rotation causes no change in the total turbulent energy.

The ratio of radial to streamwise turbulent shearing stress is given by

$$\frac{(-\overline{vw})}{(-\overline{uv})}$$

$$= \frac{\overline{v^2}(1-C_2)\partial W/\partial n - 2\Omega[(-\overline{uv})\sin\beta + (\overline{w^2}-\overline{v^2})\cos\beta]}{\overline{v^2}(1-C_2)\partial U/\partial n + (-\overline{uw})2\Omega\cos\beta} \tag{18}$$

Using a procedure similar to that employed for the derivation of Eq. (17), Eq. (18) can be written in the following form

$$\frac{(-\overline{uw})}{(-\overline{uv})} = \left(\frac{\partial W}{\partial n}\Big/\frac{\partial U}{\partial n}\right)\left(1 - \frac{(-\overline{uw})}{0.6a\overline{v^2}R_0}\right) - \frac{(-\overline{uv})\tan\beta}{0.6R_0\overline{v^2}a} - \left(\frac{\overline{w^2}}{\overline{v^2}} - 1\right)\frac{1}{0.6aR_0} + O\left(\frac{1}{R_0^2}\right) \tag{19}$$

The first three terms on the right-hand side of Eq. (19) increase the ratio of two stresses for negative values of $(-\overline{uw})$ and $(-\overline{uv})$. The fourth term also increases the ratio if $\overline{w^2}$ is larger than $\overline{v^2}$. In rotor blade boundary layers, reported in Ref. 5, $(-\overline{uw})$ is generally found to be negative and has a substantially higher value than the other two components. Thus the turbulent shearing stresses in the radial-normal plane are larger in a rotating flow than in a stationary flow. For such shear layers, the assumptions based on the stationary three-dimensional boundary layer [Eq. (14)] are no longer

valid. Structural changes are substantial enough to warrant development of separate models to include the effect of rotation.

Experimental Facilities, Program, and Accuracy

A complete description of the Axial-Flow Fan Facility, the technique and the data processing used for the measurement of rotor wakes are given in Refs. 4 and 12. Only a brief description is given here.

The rotor wake measurements were carried out with a triaxial, hot-wire probe, both rotating with the rotor and stationary behind the rotor. The rotor wake properties, both the mean flow and the turbulence characteristics, were measured in both the near wake and the far wake at various incidence angles and blade radii. The rotating and stationary probe techniques are described in Refs. 12 and 1, respectively. These techniques were modified in the present program to obtain better accuracy. The triaxial hot-wire probe and the instrumentation used in these measurements are shown in Figs. 2 and 3, respectively.

A 12-bladed, uncambered rotor was used for all wake measurements reported in this paper. The rotor blade profile is shown in Fig. 2. The rotor had the following specifications: S/c (midspan) = 0.68, tip diameter = 0.54 m, hub/tip ratio = 0.44, blade chord = 15.2 cm, stagger angle (midspan) = 45 deg. The rotor was run at 1010 rpm with the blades operating at 0, 5, 10, and 15 deg incidence angles at midspan. Most of the data presented in this paper pertain to 0 and 10 deg incidence.

A rotating probe traverse mechanism was designed and built both to rotate a probe with the rotor and to enable it to be traversed across the wake in the tangential direction while the rotor is in motion. Measurements were made by traversing the triaxial hot-wire probe across the wake at various axial and radial positions. This experimental technique provided three components of mean velocity, normal and shear turbulence stresses as well as the energy spectrum at each measurement station.

Some of the errors associated with the measurements from triaxial hot-wire probe are:

1) Inclination of the wire to the flow streamline (deviation from the cosine law).
2) Finite distance between wires (spatial resolution of the probe).
3) Finite dimensions of the hot wire (length and diameter).
4) Proximity of wire to the wall.
5) Probe body vibration for rotating hot wire.
6) Finite sampling time in the case of stationary triaxial hot-wire probe measurement.
7) Misalignment of the probe with reference to the reference axes.
8) Measurement of wire angles with reference to the coordinate system.

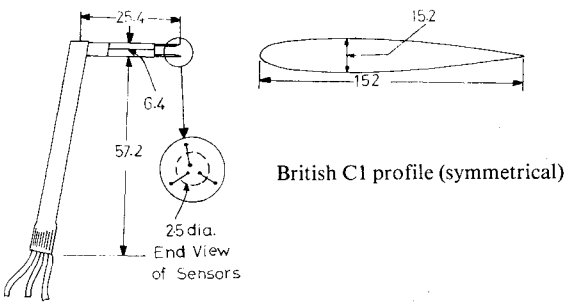

a) Triaxial hotwire probe b) Rotor blade profile

Fig. 2 Rotor blade profile and hot-wire probe used (dimensions in millimeters).

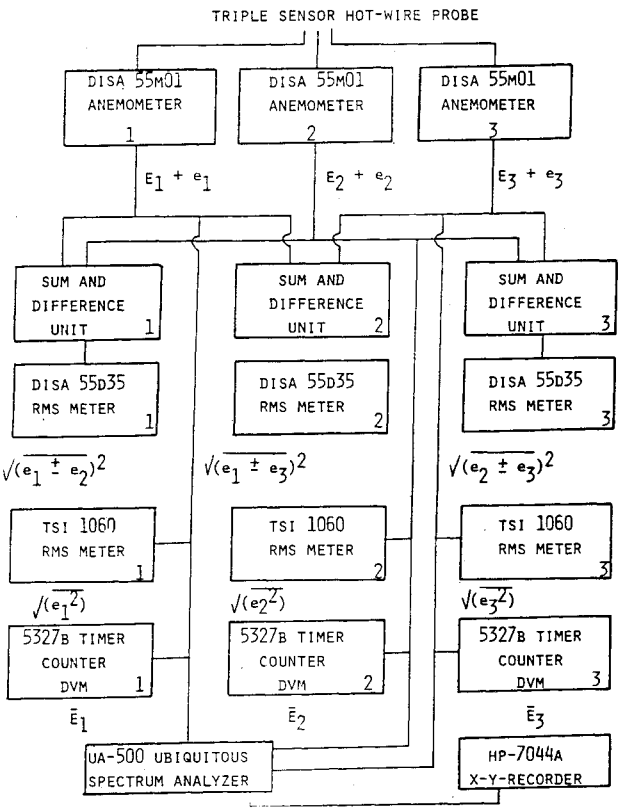

Fig. 3 Schematic of instrumentation used for rotating hot-wire probe measurement.

The last two errors and some of the other errors[5] not mentioned above can be eliminated by proper equipment and calibration procedure. Detailed procedure for estimating the various errors is given in Ref. 5. Based upon the procedure outlined in Ref. 5, an estimate of the maximum possible errors are 2% for the mean velocity, 7% for turbulent normal stress, and 15% for the turbulent shearing stress. An uncertainty bar, indicating the accuracy of the data, is shown in selected plots of the data.

Experimental Results and Correlation

The mean velocity data, profile as well as decay characteristics, are presented in Ref. 4 for two blade incidence angles (i = 0 and 10 deg) at midradius (R = 0.721). Turbulence data at these conditions are given in this paper. Only typical data are included, with a complete presentation of results given in Ref. 13. Unless otherwise stated, all the data refer to the relative frame of reference rotating with the rotor.

The turbulent normal stresses are normalized by the maximum axial velocity component in the passage at that radius, while the turbulent shearing stresses are normalized by the maximum total relative velocity at that radius.‡

Axial Component of Turbulent Normal Stresses (T_z)

Profiles of axial component of turbulent normal stresses at midradius (R = 0.721) and at rotor blade incidence angles of 0 and 10 deg are shown in Fig. 4. Turbulent normal stress has been nondimensionalized by the maximum axial velocity at that radius. The profiles of T_z in the near wake region are found to be asymmetric at all of the operating conditions. This characteristic results from the difference in the development of turbulence on the pressure and suction surfaces of the rotor blade. Symmetry in the profile of T_z is

‡In the text and nomenclature of Ref. 13 as well as an earlier version of this paper, it was incorrectly stated that the turbulent normal and shear stresses are normalized by local axial and local total velocity, respectively. The authors regret this error.

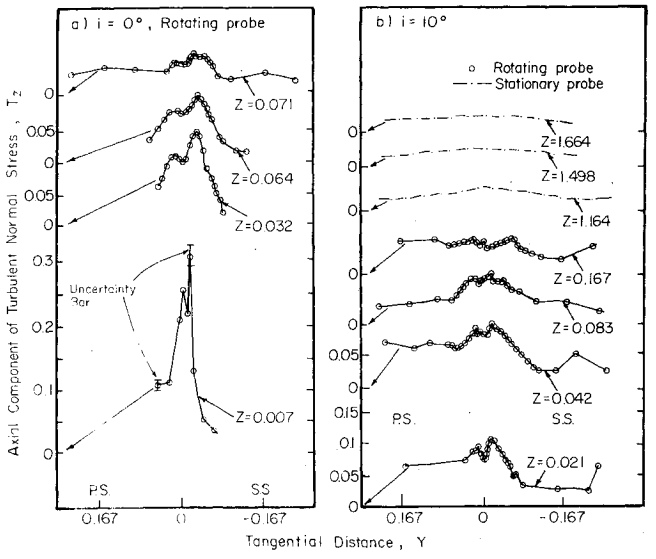

Fig. 4 Variation of axial component of turbulent normal stress (T_z) across the wake at $R = 0.721$.

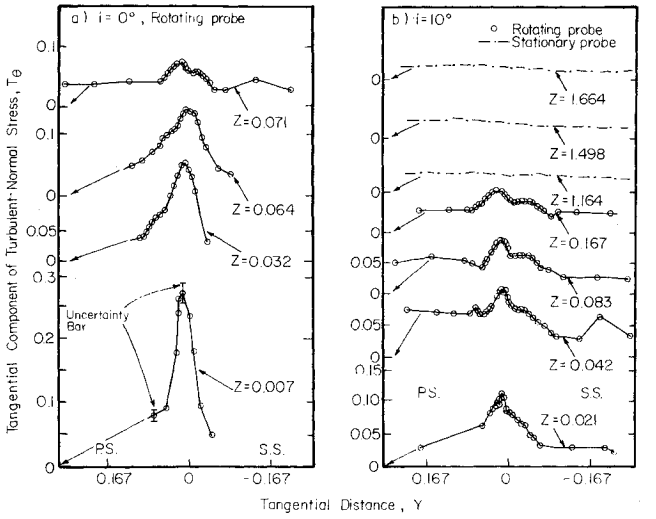

Fig. 5 Variation of tangential component of turbulent normal stress (T_θ) across the wake at $R = 0.721$.

found only at the far downstream stations ($Z > 1.0$). All of the axial-turbulent-normal stress profiles in the near-wake region have a minimum at the wake centerline. This trend is expected, since turbulent normal stresses are zero on the surface of the rotor blade trailing edge. Maximum normal stresses occur slightly away from each surface. The peak values of T_z in the near wake show a larger value on the suction side for all the rotor blade incidence angles tested. The closest measuring station is at $Z = 0.007$ (which corresponds to a downstream distance of 1.3 mm (0.05 in.) for a 15.2 cm (6 in.) chord length). The axial component of the turbulent normal stress is more than 30% at this location, indicating the highly turbulent nature of the rotor wake flow. This value decreases drastically to about 15% within 3-4% of the chord length. The variation of turbulent normal stresses across the wake is negligibly small for $Z = 1.0$.

The freestream values of the normal stresses in the axial direction, shown in Fig. 4, result from the flow conditions at the rotor inlet. An inlet turbulence level of approximately 2% does not show any appreciable amplification after moving through the blade row. Freestream turbulence level downstream of the rotor is approximately 2.5%.

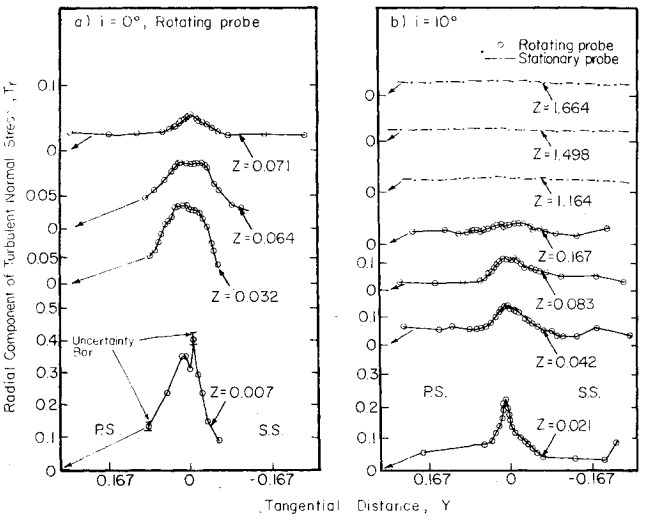

Fig. 6 Variation of radial component of turbulent normal stress (T_r) across the wake at $R = 0.721$.

Tangential (Relative) Component of Turbulent Normal Stresses

Profiles of the tangential component of turbulent normal stress are shown in Fig. 5 at midradius for rotor blade incidence angles of 0 and 10 deg. As with the axial component, the tangential components have been nondimensionalized by the maximum axial velocity at that radius.

The profile of T_θ in the near-wake region are asymmetric, exhibiting a trend similar to that found for T_z. However, unlike the axial component of normal stresses, no minimum is found at the wake centerline in the case of tangential component of normal stress. This indicates that in the inner layer of the wake a larger redistribution of turbulent energy occurs for tangential component of normal stresses near the rotor blade trailing edge than that for the axial component. The axial and tangential components of normal stresses are nearly equal at all operating conditions, with similar profile and decay characteristics.

Radial Component of Turbulent Normal Stress

The radial component of turbulent normal stress at rotor blade incidence angles of 0 and 10 deg are shown in Fig. 6. The radial component of normal stress is also normalized by the maximum axial velocity at that radii.

No minimum for T_r was found near the wake centerline at any of the near-wake measurement stations at rotor blade incidence angle of 10 deg. The minimum near the wake centerline is observed only for the 0 deg incidence operating condition at $Z = 0.007$. This indicates that the redistribution of energy for the radial component is more rapid than that for the axial component. The large redistribution seems to be comparable to that found for the tangential component. While no minimum is exhibited in the wake profiles, a larger value of the radial component of normal stress was observed on the pressure side for the near-wake profile at $i = 10$ deg, $Z = 0.021$. This characteristic is not found for the near-wake station at $i = 0$ deg, $Z = 0.042$. Data at other incidence angles do not exhibit any large peaks away from the wake centerline for the stations shown in the near-wake region.

The maximum radial component of normal stress is about 0.4 at $Z = 0.007$, $i = 0$ deg. This is about 30% higher than the corresponding axial and tangential components at this location. In the case of 10 deg incidence, the ratio of maximum-radial to maximum-axial-normal stress is nearly two and this trend persists even up to 10% chord downstream. It is thus evident that the turbulent normal stresses in the near wake are most affected by the rotation (history effect). These comments agree with the qualitative analysis presented earlier. For a 45 deg outlet angle, the streamwise component

of normal stress $\overline{u^2} \approx (\overline{w_\theta^2} + \overline{w_z^2})/2$. Hence,

$$(\overline{w^2}/\overline{u^2})_{max} = 1.33 \text{ at } Z = 0.007,\ i = 0 \text{ deg}$$

$$= 2 \text{ at } Z = 0.021,\ i = 10 \text{ deg}$$

In this particular case, both the second and the third terms on the right side of Eq. (17) contribute to the redistribution of energy. It is also evident that the "history effect" soon disappears as the wake travels downstream and a rapid trend is exhibited toward achieving isotropy (Figs. 4-6). Radial component seems to decay much more rapidly than the other two components, reaching an almost constant value at $Z \sim 1.0$.

Radial component of normal stress in the freestream is found to be approximately 3-4% for all rotor blade incidence angles tested. This is slightly larger than that found for the axial and tangential components.

Similarity in Turbulent Normal Stresses

The existence of similarity in profiles of axial, tangential, and radial components of normal stresses were examined for the outer layer of the rotor wake. The normal stresses were normalized by an extrapolated peak value of the normal stress near the wake center and the corresponding ratio in the freestream was subtracted. The distance from the wake centerline to the location where the extrapolated maximum normal stress is half is used as a characteristic length scale on the pressure and suction side (L_s and L_p, respectively). Similarity in the outer layer for the near-wake region are shown in Fig. 7. The similarity is found to exist in the outer layer of the wake at all incidence angles, except at the first measuring station for the rotating probe data at $Z = 0.021$, $i = 10$ deg, $R = 0.721$. Normal stresses seem to follow Gauss' function [$\exp(-0.693\ \eta^2)$] as in the case of mean velocity.

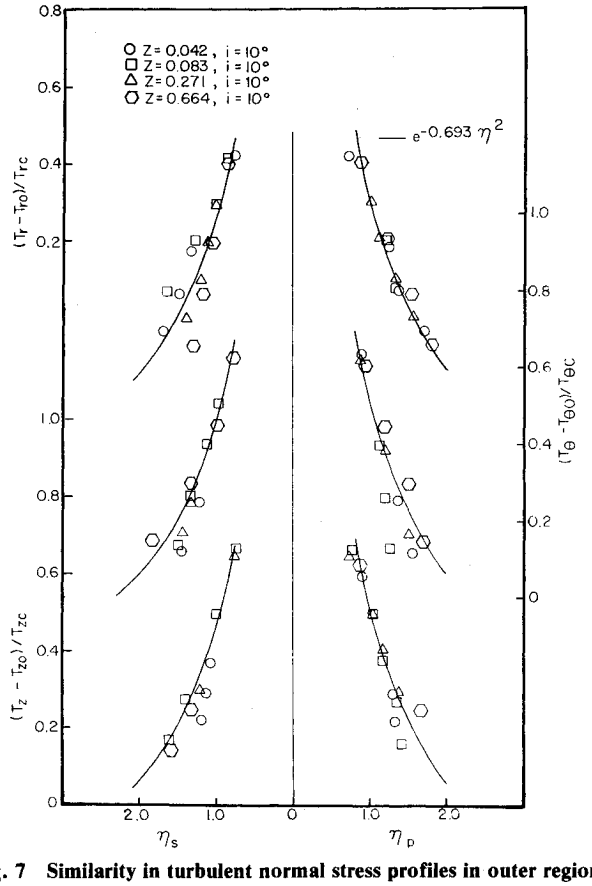

Fig. 7 Similarity in turbulent normal stress profiles in outer regions of wake at $R = 0.721$.

The normal stresses near the wake center undergo rapid changes, from the boundary-layer type to one with a minimum at the wake center to the far-wake type of distribution. The transition from the boundary-layer type of distribution to the far-wake type seem to vary from one component to the other. Hence, no attempt is made in this paper to examine the existence of similarity in the inner regions of the wake.

Decay of Turbulent Normal Stresses

Decay of maximum axial, tangential, and radial components of normal stresses in the rotor wake are shown in Fig. 8. Data are given for both the operating conditions ($i = 0$ and 10 deg) tested at midradius ($R = 0.721$). The decay is shown as a function of the streamwise distance s.

Axial, tangential, and radial components of normal stresses are found to be very large in the near-wake region for both rotor blade incidence angles. While all three components are large, radial components were found to be significantly larger than the axial and tangential components as $s/c = 0.030$ for $i = 10$ deg. However, all components have decayed to approximately the same level for $s/c > 0.4$. In the far-wake region for $s/c > 1.5$ the maximum axial, tangential, and radial components of normal stresses have decayed to levels near their freestream values. The axial and tangential normal stresses are found to be slightly greater than the radial component in this region. The effect of varying blade loading is clearly discernible in the far-wake region for $s/c > 1.5$, where larger blade loading shows increased maximum axial, tangential, and radial components of normal stresses in the wake.

In two-dimensional boundary layers and wakes the streamwise component is usually much larger than the normal and spanwise components.[14] The fact that all of the components of normal stresses in a rotor wake are of nearly equal magnitude (except at the trailing edge region where the radial component is the largest) is indicative of the effect of rotation. These observations are consistent with the qualitative analysis presented earlier and indicate a substantial change in the turbulence structure due to the rotation.

Comparison with Isolated Airfoil Wake Data

A systematic study of the wake of an isolated airfoil, which has the same profile as the rotor blade tested in this program, was carried out recently.[15] The airfoil was operated at 0, 3, 6, and 9 deg incidence angles. The lift coefficients at these incidences were nearly equal to those of the rotor blade at 0, 5, 10, and 15 deg incidences, respectively. Since the overall loading is the same, the airfoil data provide a basis for the evaluation of the effect of rotation. The turbulent normal stress profiles in s, n, r system is shown in Fig. 9 for both the rotor blade ($i = 15$ deg) and the airfoil ($i = 9$ deg) wake. The airfoil wake exhibits the conventional trend, namely,

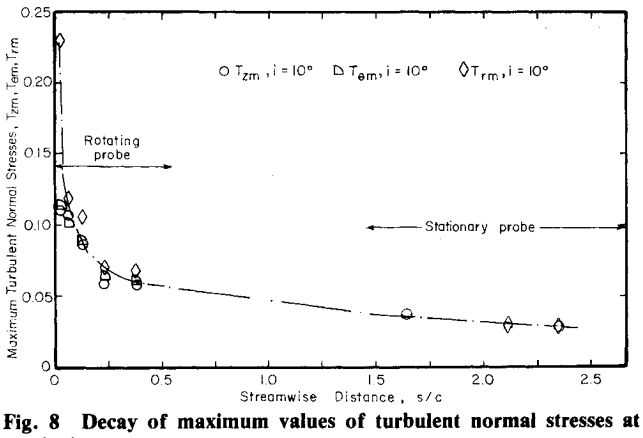

Fig. 8 Decay of maximum values of turbulent normal stresses at $R = 0.721$.

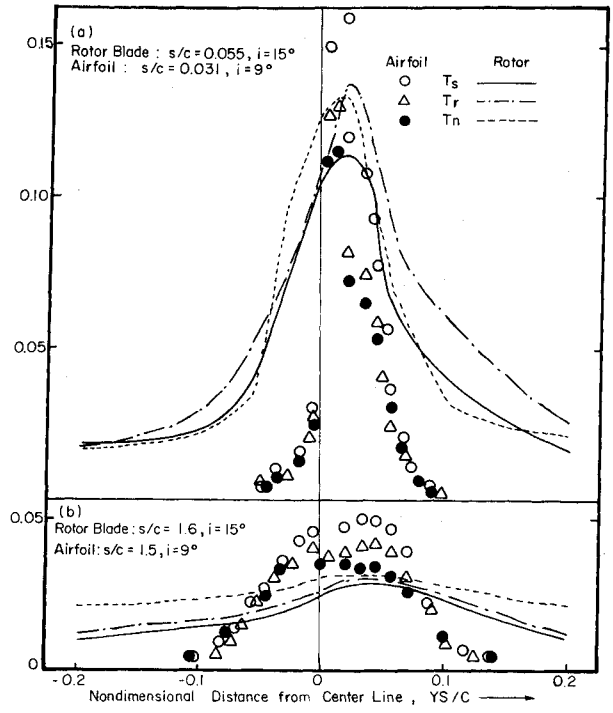

Fig. 9 Comparison between isolated airfoil and rotor wake normal stress profiles in (*s,n,r*) system.

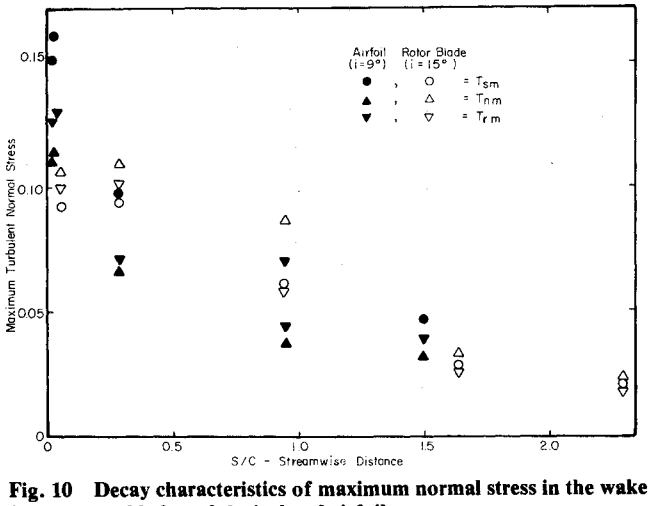

Fig. 10 Decay characteristics of maximum normal stress in the wake for the rotor blade and the isolated airfoil.

$T_s > T_r > T_n$, while the rotor wake shows that $T_r > T_s$ at all locations and $T_r > T_n$ at most locations. This result is consistent with the trend predicted by the qualitative analysis presented earlier. Both the airfoil and the rotor blade wake show a trend toward isotropy in the far wake.

The decay of the maximum turbulent normal stresses in the wake is shown in Fig.10 for the isolated airfoil and the rotor blade at $i=9$ and 15 deg, respectively. The isolated airfoil wake is highly anisotropic in the near-wake region, while the rotor wake shows a much smaller degree of anisotropy. The first measuring station for the airfoil wake was much closer than the rotor blade, therefore the observed higher intensities in the airfoil wake. Turbulent normal stresses in the isolated airfoil wake decay very rapidly in the near wake, the decay rates being different for various components. It maintains anisotropy even at $s/c=1.0$. The rotor-wake normal stresses on the other hand decay less rapidly in the near-wake region and maintain nearly equal values for all the three components.

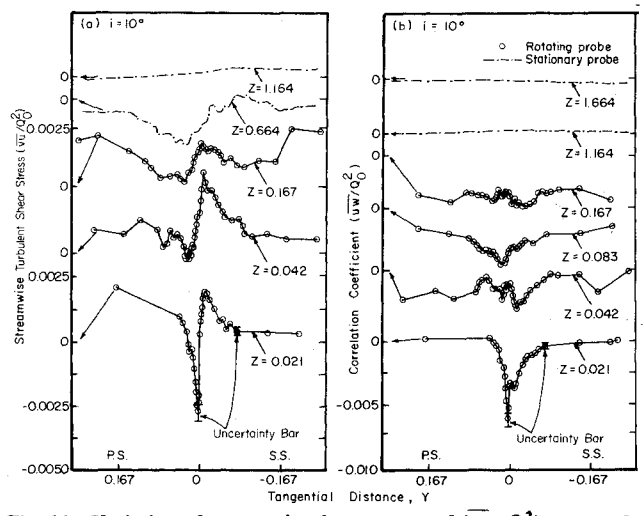

Fig. 11 Variation of streamwise shear stress and $(\overline{uw}/Q_0^2)$ across the wake at 10 deg incidence.

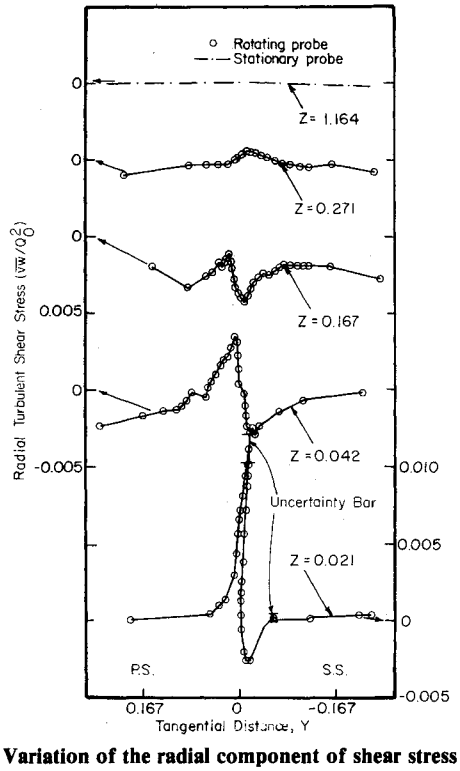

Fig. 12 Variation of the radial component of shear stress across the wake at 10 deg incidence angle.

Turbulent Shear Stresses

The shear stresses of practical interest are the streamwise and the radial components in the *s, n, r* coordinate system. Hence, the stress data are presented in the *s, n, r* system. All the shear stresses are normalized by the dynamic pressure based upon the maximum total relative velocity at that radius.

The variation of the streamwise shear stress across the wake for $i=10$ deg (rotating probe) is shown in Fig. 11. This plot shows the expected positive and negative stresses on either side of the wake centerline. This is consistent with the mean velocity distribution shown in Ref. 4. However, the location of zero streamwise shear stress does not occur at the wake centerline where $\partial O/\partial n=0$. The shear stresses near the pressure side are much higher than those on the suction side in the near wake, with this trend reversing rapidly to provide the opposite effect for $Z>0.042$. The value of shear stress is not found to be zero outside the wake, which may have been

caused by the support strut upstream of the rotor. Close to the rotor blade trailing edge, the maximum shear stresses are about the same as those for an isolated airfoil.[15]

The correlation $\overline{uw}$ plotted in Fig. 11 shows that this is larger than the streamwise shear stress and has the same sign on either side of the wake. The correlation decays very rapidly downstream.

The radial shear stress profile across the wake is shown in Fig. 12. The radial shear stresses are opposite in sign to those of the streamwise shear stress. This characteristic is consistent with the mean velocity data presented in Ref. 4, the streamwise component of velocity increasing on either side of the wake while the radial velocity decreases. The magnitude of the radial shear stress decreases more rapidly than the streamwise shear stress. The radial stresses are zero in the freestream.

As shown in Fig. 12, the maximum values of radial shear stresses at $Z=0.021$ are -0.00250 and 0.010, occurring slightly away from the wake centerline on suction and pressure sides, respectively. The corresponding values of streamwise shear stresses (Fig. 11) are $+0.002$ and -0.0025 on the suction and pressure sides, respectively. Hence, the ratio of the maximum radial to maximum streamwise shear stress is given by

$$(-\overline{vw})_m/(-\overline{uv})_m = -1.25 \text{ suction side, } Z=0.021$$

$$= -4.0 \text{ pressure side, } Z=0.021$$

The value of this ratio in the absence of rotation should be much less than unity since $W \ll U$ in Eq. (19). The effect of rotation in this case is to increase the radial shear stress or decrease the streamwise shear stress or both. This is consistent with the qualitative analysis presented earlier. The last term in Eq. (19) is negative for this case (since $\overline{w^2} > \overline{v^2}$) and its magnitude increases with increase in rotation. The first term in this equation is negative since $\partial W/\partial n$ is negative. The second term on the right-hand side containing $(-\overline{uv})$ could be positive or negative depending on the sign of $(-\overline{uv})$. For this particular case, this term is positive on the suction side (Fig. 12) and negative on the pressure side. This accounts for the higher ratio of radial to streamwise shear stress on the pressure side as compared to the suction side.

The Reynolds stress data shown in Figs. 11 and 12 must be studied with caution. The results are subject to spatial errors which may exist when using a triaxial hot-wire probe to measure shear stresses. On the basis of the error analysis described in Ref. 5, the measurements are subjected to a maximum error of 10-15%. The contribution to shear stress from eddies larger than the distance between the triaxial probe sensors is measured accurately.

The decay of the maximum turbulent shear stresses for both the rotor blade and the isolated airfoil are shown in Fig. 13.

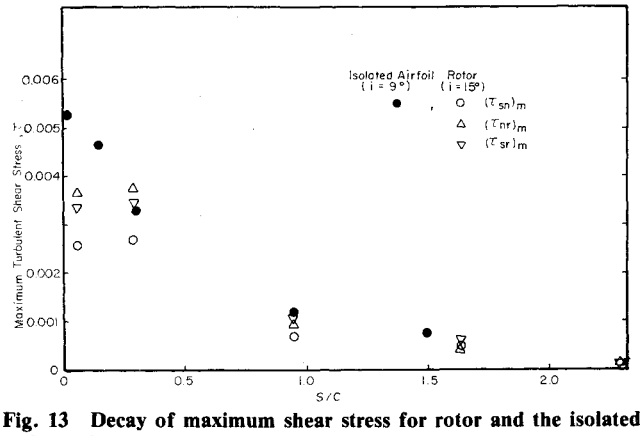

Fig. 13 Decay of maximum shear stress for rotor and the isolated airfoil wakes.

For the rotor blade at 15 deg incidence, the radial shear stress is higher than the streamwise shear stress at $s/c=0.05$. The shear stresses for the rotor wake decay slower than those for the isolated airfoil in the near wake. For $s/c>1$, they approach the same value in both cases.

Turbulent Energy Spectrum

Turbulent energy spectra taken with the spectrum analyzer are shown in Figs. 14 and 15 for measurements made in the rotating frame of reference at midradius ($R=0.721$) with the rotor blade incidence of 10 deg. For the data shown in Fig. 14 the rotating triaxial probe was located approximately at the wake centerline. The probe was located in the freestream for the energy spectrum shown in Fig. 15. The fluctuating voltages e_1, e_2, and e_3 represent measurements from the triaxial probe hot wires 1, 2, and 3, respectively. The turbulent energy is proportional to the rms value of the fluctuating voltages.

In the near-wake region ($Z=0.021$) at the wake center (Fig. 14) the turbulent energy spectrum shows a cutoff frequency of 4.0 kHz. The energy in some regions is found to be proportional to $(f)^{n_s}$. The measurements for $Z=0.021$ in Fig. 14 seem to follow a $n_s=-7/3$ law at 0.3-3.0 kHz. The eddy length in the above frequency range is approximately 0.26-2.6 cm. This eddy length size is on the order of that expected for the boundary-layer thickness at the rotor blade trailing edge. The energy spectrum shown in the far wake seems to follow an $n_s=-5/3$ law in the frequency range of 0.1-2.0 kHz. The $-5/3$ law is characteristic of isotropic turbulence. Here, the eddy size is 0.80-16.0 cm. While the smallest eddy is similar in

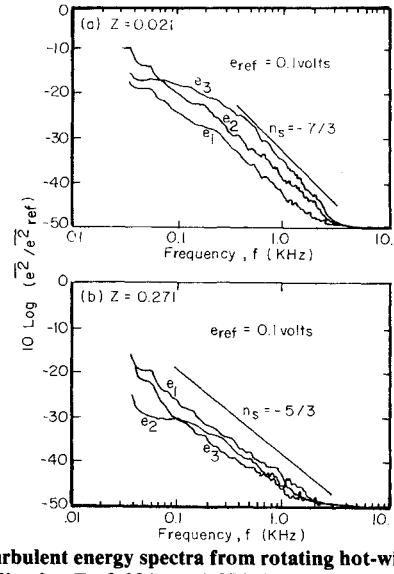

Fig. 14 Turbulent energy spectra from rotating hot-wire probe at the wake centerline for $Z=0.021$ and 0.271, $i=10$ deg, $R=0.721$.

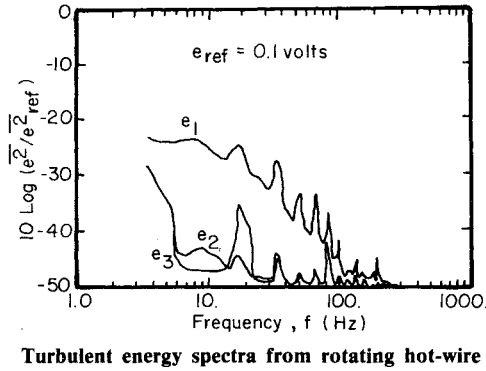

Fig. 15 Turbulent energy spectra from rotating hot-wire probe in midpassage (freestream) for $Z=0.021$, $i=10$ deg, $R=0.721$.

size in the near- and far-wake regions, the turbulence has become isotropic in the far wake.

A typical freestream turbulent energy spectrum measured by the triaxial probe is shown in Fig. 15 for $R=0.721$, $Z=0.021$ at the 10 deg incidence operating condition. The effect of the upstream strut wakes on the freestream energy spectrum is clearly seen in Fig. 15. Since the two upstream struts were located immediately next to each other, the energy spectrum shows distinct peaks at the blade passing frequency and its harmonics for one upstream disturbance. This characteristic is not evident beyond a frequency of 400 Hz. Since all the energy in the freestream appears at low frequencies, long eddies (approximately 7.0 cm) is a characteristic feature for the turbulence in this region.

Conclusions

The turbulence characteristics of a rotor blade wake has been investigated both experimentally and theoretically. The rotating triaxial probe measurements represent the first systematic turbulence data in the near-wake region of the rotor blade wake using this technique. The major conclusions derived on the basis of this investigation are:

1) The analysis indicates that the rotation has substantial influence on the structure of turbulence. The radial turbulent stresses are generally higher than those of a corresponding nonrotating case. The measured data agree with the trend predicted from this theory.

2) The radial component of normal stress is higher than the axial and tangential components in the near wake. The radial component decays more rapidly than the other two components.

3) Radial shear stresses are higher than streamwise shear stresses. This agrees with the trend predicted by the qualitative analysis.

4) There is substantial difference in the turbulence structure of the airfoil and the rotor blade wake. The anisotropy is much more predominant in the airfoil case. The near-wake decay characteristics are also different.

5) Similarity in turbulent normal stress exists in the outer layer.

6) The turbulent normal stress and the maximum shear stresses decay rapidly in the near-wake region, becoming nearly isotropic within one chord length.

7) From turbulent energy spectral measurements made in the rotating frame of reference, the turbulence in the wake is isotropic in the far-wake region following a $n_s=-5/3$ law. The turbulence followed a $n_s=-7/3$ law in the near-wake region.

Acknowledgment

This work was supported by the National Aeronautics and Space Administration, through Grant NSG 3012, with M. F. Heidmann as the technical monitor. The authors wish to thank A. K. Anand for discussions related to the analysis and A. Ravindranath for help in the experimental program. The staff of the Applied Research Laboratory provided assistance in the experimental program carried out at their Axial Flow Research Fan Facility.

References

[1] Raj, R. and Lakshminarayana, B., "Three Dimensional Characteristics of Turbulent Wakes Behind Rotors of Axial Flow Turbomachinery," *Journal of Engineering for Power*, Vol. 98, April 1976, pp. 218-228.

[2] Kerrebrock, J. L., "Small Disturbances in a Compressor with Strong Swirl," *Turbulence in Internal Flows*, S.N.B. Murthy, ed., Hemisphere Publishing Corp., Washington, D.C., 1977, p. 439.

[3] Schmidt, D. P. and Okiishi, T.H., "Multistage Wake Production, Transport and Interaction," *AIAA Journal*, Vol. 15, 1977, p. 1138.

[4] Reynolds, B., Lakshminarayana, B., and Ravindranath, A., "Characteristics of the Near Wake of a Compressor or Fan Rotor Blade," *AIAA Journal*, Vol. 17, Sept. 1979, pp. 959-967.

[5] Anand, A. K. and Lakshminarayana, B., "An Experimental Study of Three Dimensional Turbulent Boundary Layer and Turbulence Characteristics Inside a Turbomachinery Rotor Passage," *Journal of Engineering for Power*, Vol. 100, Oct. 1978, pp. 676-690.

[6] Raj, R. and Lumley, J. L., "A Theoretical Investigation on the Structure of Fan Wakes," *Journal of Fluids Engineering*, Vol. 100, 1978, pp. 113-119.

[7] Raj, R. and Lakshminarayana, B., "On the Investigation of Cascade and Turbomachinery Rotor Wake Characteristics," NASA CR 134680, Feb. 1975.

[8] Rotta, J. C., "Statistiche Theorie Nichthomogener Turbulenz," *Z. Physics*, Vol. 129, 1951, p. 517.

[9] Launder, B. E., Reece, G. J., and Rodi, W., "Progress in the Development of a Reynolds Stress Turbulence Closure," *Journal of Fluid Mechanics*, Vol. 68, Pt. 3, 1975, pp. 537-566.

[10] Pope, S. B. and Whitelaw, J. H., "The Calculation of Near Wake Flows," *Journal of Fluid Mechanics*, Vol. 73, 1976, pp. 9-32.

[11] Nash, J. F. and Patel, V. C., *Three Dimensional Turbulent Boundary Layers*, SBC Books, Inc., 1972.

[12] Gorton, C. A. and Lakshminarayana, B., "A Method of Measuring the Three Dimensional Mean Flow and Turbulence Quantities Inside a Rotating Turbomachinery Passage," *Journal of Engineering for Power*, Vol. 98, No. 2, 1976, pp. 137-146.

[13] Reynolds, B., "Characteristics of Lightly Loaded Rotor Blade Wakes," M.S. Thesis, Dept. of Aerospace Engineering, The Pennsylvania State University, University Park, Pa., 1978, (NASA CR 3188, Oct. 1979).

[14] Hinze, J. O., *Turbulence*, McGraw-Hill, New York, 1975.

[15] Hah, C. and Lakshminarayana, B., "Mean Velocity and Turbulence Characteristics of an Isolated Airfoil Wake," (to be submitted to the *Journal of Fluid Mechanics*).